Physics of the Solid State, Vol. 47, No. 4, 2005, pp. 678–683. Translated from Fizika Tverdogo Tela, Vol. 47, No. 4, 2005, pp. 654–659.

MAGNETISM AND FERROELECTRICITY

Transition between Incommensurate Phases Accompanied by Reversal of the Magnetic Structure Vector in CuB_2O_4

S. N. Martynov

Kirensky Institute of Physics, Siberian Division, Russian Academy of Sciences, Akademgorodok, Krasnoyarsk, 660036 Russia

e-mail: unonav@iph.krasn.ru

Received June 22, 2004

Abstract—The incommensurate magnetic state of copper metaborate CuB_2O_4 is studied in the temperature range $2 < T < 12$ K. Competition between frustrated and non-frustrated antisymmetric exchange interactions is shown to cause the magnetic structure vector to reverse at $T = 10$ K. © *2005 Pleiades Publishing, Inc.*

1. INTRODUCTION

Recent intensive studies on the magnetic structure of CuB_2O_4 have revealed several different types of magnetic ordering, with phase transitions between them occurring under variation of either the temperature or magnetic field [1–5]. The variety of magnetic structures is due to the fact that, in copper metaborate, there are two distinct subsystems of magnetic Cu^{2+} ions in which the ions occupy different crystallographic positions and interact differently both within a subsystem and between them. The exchange interaction between the copper ions occupying the 4*b* sites with S_4 symmetry forms a three-dimensional magnetic subsystem *A* with a Néel temperature $T_{N1} = 20$ K, below which the average magnetic moment at *A* sites grows rapidly and reaches $0.94\mu_B$ at $T = 2$ K. The magnetic moments of subsystem *B* in the 8*d* sites with C_2 symmetry reach only $0.54\mu_B$ at the above temperature. The low magnitude of the magnetic moment at $T \longrightarrow 0$ K indicates quasi-low-dimensionality [6, 7] and/or a frustrated nature [8] of the main exchange interactions. Analysis of the exchange interactions in subsystem *B* has shown that there are two distinct competing AFM interactions between nearest and next-to-nearest neighbors and that these interactions create zigzag ladder chains along the tetragonal axis (a quasi one-dimensional magnetic structure) [9]. The existence of quasi-one-dimensional fluctuations caused by short-range correlations in CuB_2O_4 is also supported by strong diffuse neutron scattering observed both above and below the Néel temperature [3]. Therefore, the main distinction between the magnetic subsystems is the difference in the magnetic dimensionality of the main interactions within the subsystems. Analysis of the spin excitation spectra of each subsystem with inclusion of these interactions leads to the conclusion that the interactions between the subsystems have little effect on the dynamic properties of copper metaborate at $T = 12$ K [9, 10]. The reason for the interactions between the two subsystems being weak is the geometry of the intersubsystem exchange bonds. All paths of the indirect exchange interactions link an ion of one subsystem to two ions of another subsystem that belong to different antiferromagnetic (AFM) sublattices. This leads to fully frustrated exchange interaction between the subsystems when there is an AFM ordering within them. Ladder chains interact in a similar fashion, so the subsystem *B* becomes quasi-low-dimensional. An incommensurate magnetic structure is observed in CuB_2O_4 below $T_s \approx 10$ K with the wave vector directed along the tetragonal axis [3, 4]. The magnitude of the wave vector grows steadily with decreasing temperature and reaches 0.15 relative lattice units (rlu) at $T = 2$ K. According to a phenomenological analysis of the transition into the incommensurate phase, the Lifshitz invariant plays an important part in its formation [3, 4, 11]. From the field dependence and resonance properties of CuB_2O_4, it follows that a long-period incommensurate magnetic structure also exists in the high-temperature phase in the range $10 < T < 20$ K [4, 5]. In this paper, we analyze the magnetic structure of copper metaborate using a simple-helix model in the range $2 \text{ K} < T < 12$ K in order to determine the microscopic mechanism and type of transition between these two phases.

2. CRYSTAL STRUCTURE AND EXCHANGE INTERACTIONS

The crystal structure of CuB_2O_4 (Fig. 1) has been studied in detail in several papers [3, 4, 12]. The exchange interactions are due to hybrid *s–p* orbitals of tetrahedrons formed by oxygen atoms around boron atoms (the indirect superexchange chains Cu–O–B–O–Cu). Aside from the AFM exchange interactions within each subsystem, which were considered in [9, 10], we take into account the following: (i) the AFM exchange

1063-7834/05/4704-0678$26.00 © 2005 Pleiades Publishing, Inc.

interaction between the subsystems (Fig. 1, solid lines), (ii) the exchange interaction between the ladders of subsystem *B* (dashed lines), and (iii) antisymmetric exchange interactions both between the subsystems and within them. In case (i), the AFM exchange interaction between the subsystems J_{ab}^{m} is realized along three different paths connecting Cu^{2+} ions separated by $\Delta z = c/8$, $3c/8$, and $5c/8$ along the tetragonal *c* axis. The exchange interaction between neighbors that are the most closely spaced along *z* and are remote in the *ab* plane is realized via the single Cu–O–B–O–Cu chain shown by single solid lines in Fig. 1. Two other exchange interactions are realized via the "one-and-a-half" chain shown by double solid lines in Fig. 1. The latter chain is displayed separately in Fig. 1. In case (iii), the exchange interaction between the ladder chains of subsystem *B* is realized via similar one-and-a-half chains and the local environment of interacting Cu^{2+} ions roughly comprises the mutually orthogonal squares formed by oxygen ions, similar to the case of the exchange between the subsystems. All exchange interactions of types (i) and (ii) are fully frustrated when the magnetic moments within the subsystems have AFM ordering. Symmetry analysis of the structure of CuB_2O_4 [11] shows that two distinct types of antisymmetric exchange interaction are possible in case (ii) [13, 14]. One type causes the magnetic moments of the AFM sublattices to be tilted and results in a weak ferromagnetic moment. This type of interaction occurs between the nearest neighbors in subsystem *A* (D_a). The other type of antisymmetric exchange interaction results in a turn in the interacting moments, which leads to the appearance of a helical structure. This type of interaction can occur between the subsystems (D_{ab}) and between the nearest and next-to -nearest neighbors within the ladders (D_{b1}, D_{b2}). The D_{b2} interaction only results in inessential renormalization of the analogous exchange interaction D_{b1}, so it is ignored below. Therefore, the exchange Hamiltonian in CuB_2O_4 can be written as

$$H = \sum_{a}\sum_{ii'} J_a^{\alpha} S_i^{\alpha} S_{i'}^{\alpha} + J_{b1}\sum_{j} \mathbf{S}_j \mathbf{S}_{j+1} + J_{b2}\sum_{j} \mathbf{S}_j \mathbf{S}_{j+2}$$
$$+ \sum_{m}\sum_{ij} J_{ab}^{m} \mathbf{S}_i \mathbf{S}_j + J_{b3}\sum_{jj'} \mathbf{S}_j \mathbf{S}_{j'} + D_a^{z}\sum_{ii'} (-1)^{i} [\mathbf{S}_i \times \mathbf{S}_{i'}]_z \quad (1)$$
$$+ D_{b1}^{z}\sum_{j} [\mathbf{S}_j \times \mathbf{S}_{j+1}]_z + \sum_{m}\sum_{ij} D_{ab}^{m,z} [\mathbf{S}_i \times \mathbf{S}_j]_z.$$

The first term in Eq. (1) describes easy-plane anisotropy in subsystem *A* [10]. Since all interactions occur between the magnetic moments positioned in various tetragonal planes ($\Delta z \neq 0$), the interacting spins are numbered along the tetragonal axis.

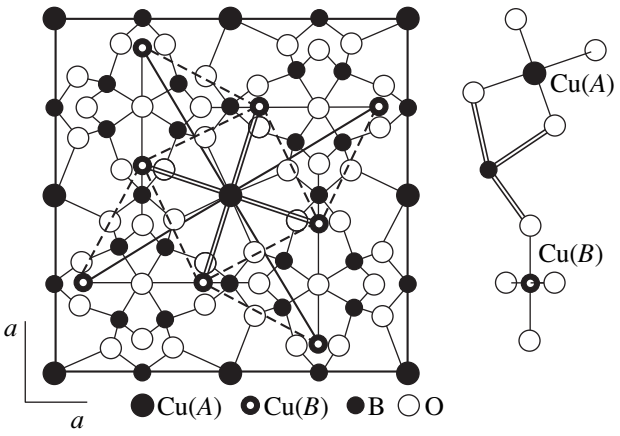

Fig. 1. CuB_2O_4 crystal structure (projection onto the tetragonal plane). The intersubsystem exchange interaction $J_{ab}^{2,3}$ is shown to the right.

3. LOCAL EXCHANGE FIELDS

If the transition of an antiferromagnet to an ordered phase is not accompanied by doubling of the elastic neutron scattering reflections, the number of possible orientations of magnetic moments of the antiferromagnet coincides with the number of magnetic ions in its unit cell. The unit cell of CuB_2O_4 has six magnetic ions: two ions in subsystem *A* and four ions in subsystem *B*. In order to describe a simple helix, we need to introduce the angle 2δ corresponding to the rotation of magnetic moments in passing from one unit cell to the next along the direction of the incommensurability vector. Since the Hamiltonian is invariant under rotation of the crystal in the tetragonal plane, the origin for the angles in the plane can be chosen arbitrarily. Consequently, we need six variables to describe the simple helix structure in CuB_2O_4. Among them, five angular variables for one unit cell can be found from the condition that the components of the total average field that are normal to the equilibrium orientation of each of the moments must be zero. The sixth variable, the helix angle, can be found by minimizing the total free energy of the unit cell with respect to this variable. A simplified diagram of the exchange interactions is shown in Fig. 2.

We choose a local coordinate frame for each of the moments such that its **Z** axis is along the tetragonal axis. The direction of the projection of the equilibrium moment $\mathbf{S}_i$ onto the tetragonal *xy* plane is chosen to be another coordinate axis, $\mathbf{X}_i$. Now, we express the Hamiltonian in terms of the orientation angles of the local coordinate axes. For each pair of interacting spins, we get

$$S_i^x S_j^x + S_i^y S_j^y = (S_{xi}S_{xj} + S_{yi}S_{yj})\cos(\alpha_i - \alpha_j)$$
$$+ (S_{xi}S_{yj} - S_{yi}S_{xj})\sin(\alpha_i - \alpha_j),$$

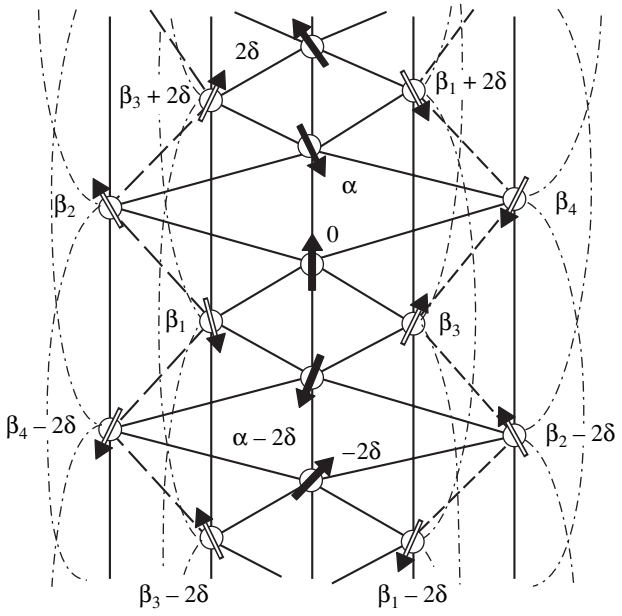

Fig. 2. Simplified diagram of the exchange interactions. Vertical lines represent the J_a exchange interaction in subsystem A with the coordination number $z_a = 4$ (the central line) and the J_{b1} exchange interaction in four ladders passing through all unit cells of the crystal (coordination number $z_b = 2$). Slanting lines represent the J^1_{ab} exchange interaction between the subsystems and half of the J_{b3} exchange interactions between ladders (dashed lines). Dash-dotted lines represent the J_{b2} exchange interaction. The $J^{2,3}_{ab}$ exchange interactions are not shown. Arrows in the chart represent the directions of magnetic moments projected onto the tetragonal plane. Each arrow corresponds to a layer of moments (z = const) changing its orientation along the tetragonal (z) axis, which coincides with the vertical axis of the chart. An arbitrary spin of subsystem A $\alpha_0 = 0$ is chosen as a reference for the angles (the central spin in the chart).

$$S_i^x S_j^y - S_i^y S_j^x = -(S_{xi}S_{xj} + S_{yi}S_{yj})\sin(\alpha_i - \alpha_j) + (S_{xi}S_{yj} - S_{yi}S_{xj})\cos(\alpha_i - \alpha_j).$$

In the local reference frame, we have $\langle S_{yi}\rangle \equiv 0$. In the mean-field approximation, coefficients h_y^i of the transverse components S_{yi} must vanish after summing the contributions from nonzero components of the average spins $\langle S_{xi}\rangle$ over interactions included in Eq. (1) [15]:

$$h_y^0 = -2S_{ax}\cos\delta(J_a\sin(\gamma-\delta) - D_a\cos(\gamma-\delta)) - S_{bx}\left(f_1\cos\frac{\beta_1-\beta_3}{2} + f_2\cos\frac{\beta_2-\beta_4}{2}\right) \equiv 0,$$

$$h_y^{\beta 1} = -S_{bx}[\sin(\beta_1-\beta_3)(J_{b1}\cos2\delta + D_{b1}\sin2\delta) + 2J_{b3}\cos\delta(\sin(\beta_1-\beta_2+\delta) + \sin(\beta_1-\beta_4+\delta))] + S_{ax}\cos(\beta_1 - 0.5\gamma + \delta)f_3(\gamma,\delta) \equiv 0,$$

$$h_y^{\beta 2} = -S_{bx}[\sin(\beta_2-\beta_4)(J_{b1}\cos2\delta + D_{b1}\sin2\delta) + 2J_{b3}\cos\delta(\sin(\beta_2-\beta_1-\delta) + \sin(\beta_2-\beta_3-\delta))] + S_{ax}\cos(\beta_2 - 0.5\gamma + \delta)f_4(\gamma,\delta) \equiv 0,$$

$$h_y^{\beta 3} = h_y^{\beta 1}(\beta_1 \longleftrightarrow \beta_3),$$

$$h_y^{\beta 4} = h_y^{\beta 2}(\beta_2 \longleftrightarrow \beta_4),$$

$$f_1(\gamma,\delta) = J^1_{ab}\cos(0.5\gamma-\delta) + J^2_{ab}\cos(0.5\gamma+\delta) + J^3_{ab}\cos(0.5\gamma-3\delta) - D^1_{ab}\sin(0.5\gamma-\delta) + D^2_{ab}\sin(0.5\gamma+\delta) - D^3_{ab}\sin(0.5\gamma-3\delta),$$

$$f_2(\gamma,\delta) = J^1_{ab}\cos(0.5\gamma) + J^2_{ab}\cos(0.5\gamma-2\delta) + J^3_{ab}\cos(0.5\gamma+2\delta) + D^1_{ab}\sin(0.5\gamma) - D^2_{ab}\sin(0.5\gamma-2\delta) + D^3_{ab}\sin(0.5\gamma+2\delta),$$

$$f_3(\gamma,\delta) = -J^1_{ab}\sin(0.5\gamma-\delta) - J^2_{ab}\sin(0.5\gamma+\delta) - J^3_{ab}\sin(0.5\gamma-3\delta) - D^1_{ab}\cos(0.5\gamma-\delta) + D^2_{ab}\cos(0.5\gamma+\delta) - D^3_{ab}\cos(0.5\gamma-3\delta),$$

$$f_4(\gamma,\delta) = J^1_{ab}\sin(0.5\gamma) + J^2_{ab}\sin(0.5\gamma-2\delta) + J^3_{ab}\sin(0.5\gamma+2\delta) - D^1_{ab}\cos(0.5\gamma) + D^2_{ab}\cos(0.5\gamma-2\delta) - D^3_{ab}\cos(0.5\gamma+2\delta),$$

where $\gamma = \alpha - \pi$ is the angle of deviation of the magnetic moments of subsystem A from the AFM orientation within each unit cell. Here and henceforth, $S_{ax,\,bx}$ denote the average x components of the spins of the subsystem. Therefore, all angles in the basic unit cell are expressed in terms of δ. The mean fields acting on the x components of the spins of each subsystem are given by

$$h_{ax} = -\frac{S_{ax}}{2}\left[4\cos(\gamma-\delta)(J_a\cos\delta + D_a\sin\delta) + \frac{(J_{b1}\cos2\delta + D_{b1}\sin2\delta)(f_3^2 + f_4^2) + 2J_{b3}\cos\delta f_3 f_4}{(J_{b1}\cos2\delta + D_{b1}\sin2\delta)^2 - (J_{b3}\cos\delta)^2}\right], \quad (2)$$

$$h_{bx} = -S_{bx}(J_{b1}\cos2\delta + D_{b1}\sin2\delta - J_{b2}\cos4\delta),$$

because of the condition imposed on γ:

$$2\cos\delta(J_a\sin(\gamma-\delta) - D_a\cos(\gamma-\delta))((J_{b1}\cos2\delta + D_{b1}\sin2\delta)^2 - (J_{b3}\cos\delta)^2) - (J_{b1}\cos2\delta + D_{b1}\sin2\delta)(f_1f_3 - f_2f_4) - J_{b3}\cos\delta(f_1f_4 - f_2f_3) = 0.$$

Thus, in the mean-field approximation, the intersubsystem interaction in the simple-helix model results in

an additional longitudinal field acting on spins of subsystem A (the second term in Eq. (2)) and, furthermore, the decrease in the intrasubsystem exchange field is compensated for by a tilt of the magnetic moments in subsystem B ($\beta_1 - \beta_3 \neq \pi \neq \beta_2 - \beta_4$). The subsystems remain quasi-independent, because the additional effective fields within each subsystem do not depend directly on the magnetization of the other subsystem.

4. FREE ENERGY

In the mean-field approximation, the minimum of the free energy

$$F = -k_B T \ln \mathrm{Sp}\{\exp(-\beta H)\}$$

can be easily found by fixing the magnitude of the average spin at sites of each subsystem and varying the total energy with respect to the helix pitch. Possible influence of the pitch variation on the spin magnitude is disregarded. This simplification is equivalent to the approximation of the fixed magnitude of the order parameter, which is widely used for phenomenological analysis of incommensurate structures [16]. In the temperature range of interest, the magnetic moments of subsystem A are oriented approximately in the tetragonal plane; their magnitude varies between $0.86\mu_B$ and $0.94\mu_B$ and will be assumed to be constant and equal to $0.9\mu_B$. The magnitude of the magnetic moments of subsystem B varies from $0.2\mu_B$ at $T = 12$ K to $0.54\mu_B$ at $T = 2$ K. In order to describe its variation with temperature between these limits, we consider subsystem B as a set of two-level single-site spin $S = 1/2$ states. The corresponding wave functions for the ground and excited states are given by

$$\Psi_{0i} = C_0^+ |+\rangle_i \Psi^+_{0,N-1} + C_0^- |-\rangle_i \Psi^-_{0,N-1},$$

$$\Psi_{ei} = C_e^+ |+\rangle_i \Psi^+_{e,N-1} + C_e^- |-\rangle_i \Psi^-_{e,N-1}$$

for each spin subjected to the mean field of all other spins. Here, $C^{+,-}_{0,e}$ are the probability amplitudes of the ground and excited states of the spin S_i with "+" and "–" projection to the local axis, respectively, and $\Psi^{+,-}_{0,e,N-1}$ are the corresponding normalized wave functions of the states of all other $N-1$ spins. The average values of the spin at a site in each of the states are

$$S_0 = S_b(T \longrightarrow 0) = \frac{1}{2}(|C_0^+|^2 - |C_0^-|^2),$$

$$S_e = \frac{1}{2}(|C_e^+|^2 - |C_e^-|^2)$$

and differ from the values for the free ion $S = \pm 1/2$. The temperature dependence of the spin can be found to be

$$S_b(T) = \frac{S_0 \exp(\Delta E/2k_B T) + S_e \exp(-\Delta E/2k_B T)}{\exp(\Delta E/2k_B T) + \exp(-\Delta E/2k_B T)},$$

where ΔE is the level splitting in the mean field. From the condition $\lim S_b (T \longrightarrow \infty) = 0$, we get $S_0 = -S_e$ and the energy is $\Delta E/2 = S_0 h_b$. Finally, we arrive at the well-known expression for a two-level system in the mean field h_b:

$$S_b = S_0 \tanh \frac{S_0 h_b}{k_B T}.$$

For an experimentally observed long-period helix [4], the difference in the temperature dependence between the mean field h_b and the average spin due to the helical in-plane rotation of the moments (the term in parentheses in the second of equations (2) depends on δ) is small and can be neglected. Thus, the temperature dependence of the average magnetization at sites in subsystem B can be described with sufficient accuracy in terms of the temperature of the onset of macroscopic magnetization in subsystem B [15]:

$$m_b = m_b^0 \tanh \frac{m_b T_{N2}}{m_b^0 T}, \quad (3)$$

$$k_B T_{N2} = S_0^2 (J_{b1} - J_{b2}). \quad (4)$$

For the magnetization values cited above, we get $m_b^0 = 0.54\mu_B$ and $T_{N2} = 12.6$ K.

The angle the magnetic moments of the subsystem B make with the tetragonal axis increases from a small value to $\Theta_0 \approx \pi/2.7$ as the temperature decreases to $T = 2$ K [3]. We do not consider the mechanism behind this change in direction because, in this paper, we disregard anisotropy of subsystem B for the sake of simplicity. The variation in the orientation of the moments in system B with temperature is described by a power law,

$$\Theta = \Theta_0 (1 - T/T^*)^n \quad (5)$$

with $n = 1$ (linear dependence) or $n = 0.5$ (which corresponds to the variation in the order parameter for the second-order orientation phase transition in a three-dimensional system [17]). In both cases, the temperature of the onset of reorientation, according to experiment [3], is close to T_{N2}: $T^* = 12.4$ K ($n = 1$) and 12.3 K ($n = 0.5$). This simple approximation gives only a qualitative description of $k(T)$ for intermediate temperatures.

Varying the free energy with respect to the helix pitch in one unit cell of the crystal reduces to varying the longitudinal mean fields

$$\delta F_1 = 2S_{ax}\delta h_{ax} + 4S_b \delta h_b.$$

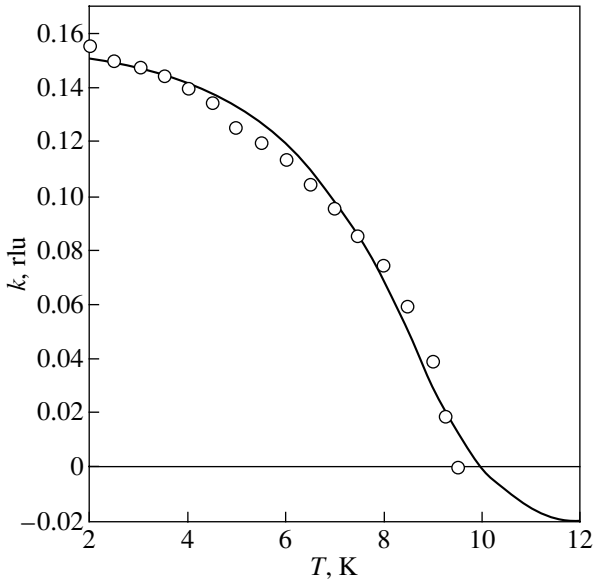

Fig. 3. Temperature dependence of the incommensurability vector $k(T)$. Dots are experimental data [4] and the solid line is the mean-field approximation in the simple-helix model with a linear temperature dependence of the moment direction in subsystem B: $\Theta = \Theta_0(1 - T/T^*)$. Parameter values: $J_{b1} = 234$ K, $J_{b2} = 59.4$ K, $J_{ab} = 67.5$ K, $D_{b1} = 21.1$ K, $D_{ab} = 5.6$ K, $D_a = 1.1$ K, and $J_{b3} = 0$ K.

The component h_{bz} is invariant relative to helical rotation of the moments in the tetragonal plane:

$$h_b = \sqrt{h_{bx}^2 + h_{bz}^2}, \quad \delta h_b = \frac{h_{bx}\delta h_{bx}}{\sqrt{h_{bx}^2 + h_{bz}^2}} = \sin\Theta\delta h_{bx}, \quad (6)$$
$$S_{bx} = S_b\sin\Theta, \quad \Delta F_1 = 2S_{ax}\delta h_{ax} + 4S_{bx}\delta h_{bx}.$$

Within our approximations, the part of the free energy that changes with the helix pitch depends only on the x components of spins of the subsystems and its variation with temperature is determined by the temperature dependence of the x component of subsystem B.

Using Eqs. (2) for the fields and Eqs. (3) and (5) for the temperature dependences of the magnitude and direction of the magnetic moment, we numerically minimize the part of the free energy that depends on the helix angle,

$$F_1(\delta) = 2S_{ax}h_{ax}(\delta) + 4S_{bx}h_{bx}(\delta), \quad (7)$$

and obtain the temperature dependence of the simple-helix vector $k(T)$.

5. RESULTS AND DISCUSSION

The best agreement between the calculated temperature dependence of the incommensurate structure vector and elastic neutron scattering data is obtained for $n = 1$ and

$$2J_{ab}^1 = J_{ab}^2 = J_{ab}^3 = J_{ab}, \quad 2D_{ab}^1 = D_{ab}^2 = D_{ab}^3 = D_{ab}$$

(Fig. 3). The J_{b3} interaction between ladders has almost no effect on $k(T)$, so it was assumed to be zero in calculations. The main feature of the temperature dependence of the helix vector is the reversal of the vector sign at $T_s \approx 10$ K; i.e., the left-handed helix is replaced by a right-handed one. This transition can be either continuous or discontinuous, depending on the relationship between the next-to-nearest neighbor exchange interaction in subsystem B (which is responsible for the potential with two minima as a function of δ) and the Dzyaloshinskiĭ interaction. The exchange constant of subsystem A in the Hamiltonian was assumed to be equal to $J_a = 45$ K, a value obtained from analyzing the spin-wave spectrum and the Néel temperature T_{N1} [10]. The magnitudes of exchange interactions in subsystem B were varied in a wide range subject to Eq. (7). For the ratio of the next-to-nearest and nearest neighbor exchange interactions, we obtained $J_{b2}/J_{b1} = 0.25$, which is close to the value of 0.26 obtained in [9]. However, the magnitudes of each of the interactions are almost one order of magnitude greater than the results from [9], because the linear theory of spin waves employed in [9] does not take into account the decrease in the saturation value of the moment due to quasi-low-dimensionality of the system. Consequently, the exchange interactions that were derived through comparison with the spin excitation energy given by inelastic neutron scattering measurements are underestimated. The saturation value of the site moment of $S = 1/2$ chains in the mean field of interchain interaction is related to the ratio of the intrachain interaction and the Néel temperature [6, 7]. This relation shows how much the Néel temperature of a quasi-one-dimensional system differs from the Néel temperature of the corresponding three-dimensional system. In our case, it is convenient to compare subsystems A and B, for which we obtain

$$K = \frac{z_a J_a T_{N2}}{z_b(J_{b1} - J_{b2})T_{N1}} \approx 0.33.$$

This value is in good quantitative agreement with the theoretical result from [6] for $m_b^0 = 0.54\mu_B$ [7]. The maximum value of the incommensurability vector $k = 0.15$ rlu at $T = 2$ K is determined by the combined effect of the next-to-nearest-neighbor AFM exchange interaction J_{b2} and the Dzyaloshinskiĭ nearest neighbor interaction D_{b1} in subsystem B. As the temperature increases, the contribution from subsystem B to the free energy decreases as $(m_b^0)^2$ [10] and the incommensurability vector reverses at the point where the interactions D_{b1} and D_{ab} are balanced. Although these antisymmetric exchange interactions are of the same sign, the con-

tributions from them are different because the former interaction couples the moments of different AFM sublattices, while the latter couples the moments of a subsystem to the moments of both sublattices of the other subsystem, i.e., with the weak ferromagnetic moment. The ratios of these interactions to the corresponding AFM exchange interactions are similar, 0.9×10^{-1} and 0.8×10^{-1}. The sign of the Dzyaloshinskiĭ exchange interaction between spins of subsystem A is unknown. If $D_a < 0$, this interaction promotes the $k < 0$ phase and the agreement with the experimental data is achieved at a lower value of D_{ab}.

Note that, near the temperature where k changes sign, the simple-helix model is inadequate and cannot describe a longitudinal modulation of magnetization [11] or a complex magnetic structure of the soliton-lattice type. The existence of such a structure is indicated by the satellite peaks observed in neutron scattering near T_s [2]. Clearly, the approximation of the magnetization by the Brillouin function, Eq. (6), is well-founded only for $T < 12$ K, where the magnetization of subsystem B is mainly determined by the intrasubsystem exchange interactions J_{b1} and J_{b2}. At $T > 12$ K, the intersubsystem exchange interaction plays an important part and the magnetization of subsystem B does not vanish until the long-range order disappears in subsystem A at $T_{N1} = 20$ K. For small values of m_b, there is a solution for the unit cell angles that gives a longitudinal field differing from Eq. (2). Therefore, the structure vector found by us, $k(T = 12\ \text{K}) \sim 0.02$ rlu, is only an upper bound estimation. However, the growth of the wave vector in magnitude with the temperature increasing from T_s is indirectly supported by the temperature–field phase diagram [4, 5]. The fact that the field destroying the incommensurate structure increases with temperature indicates that k at $H = 0$ also increases.

6. CONCLUSIONS

We can draw two main conclusions from the results obtained in this paper. (1) The magnitudes of exchange interactions, the temperature of the onset of macroscopic magnetization, and the saturation moment of subsystem B correspond to the quasi-one-dimensional type of interactions in this subsystem. (2) The competition between the frustrated and nonfrustrated antisymmetric exchange interactions causes the magnetic structure vector to reverse sign at $T_s \approx 10$ K.

6. ACKNOWLEDGMENTS

The author is grateful to V.I. Zinenko, M.A. Popov, G.A. Petrakovkiĭ, and A.I. Pankrats for helpful discussions.

This work was supported by the Russian Foundation for Basic Research, project no. 03-02-16701.

REFERENCES

1. G. Petrakovskii, D. Velikanov, A. Vorotinov, *et al.*, J. Magn. Magn. Mater. **205** (1), 105 (1999).
2. B. Roessli, J. Schefer, G. Petrakovskii, *et al.*, Phys. Rev. Lett. **86** (9), 1885 (2001).
3. M. Boehm, B. Roessli, and J. Schefer, Phys. Rev. B **68**, 024405 (2003).
4. G. A. Petrakovskii, A. I. Pankrats, M. A. Popov, *et al.*, Low Temp. Phys. **28** (8–9), 606 (2002).
5. A. I. Pankrats, G. A. Petrakovskiĭ, M. A. Popov, *et al.*, Pis'ma Zh. Éksp. Teor. Fiz. **78** (9–10), 1058 (2003) [JETP Lett. **78**, 569 (2003)].
6. H. J. Schultz, Phys. Rev. Lett. **77** (13), 2790 (1996).
7. K. M. Kojima, Y. Fudamoto, M. Larkin, *et al.*, Phys. Rev. Lett. **78** (9), 1787 (1997).
8. E. M. Lifshitz and L. P. Pitaevskiĭ, *Statistical Physics* (Fizmatlit, Moscow, 2001; Butterworth, Oxford, 1998), Part 2.
9. S. Martynov, G. Petrakovskii, B. Roessli, *et al.*, J. Magn. Magn. Mater. **269**, 106 (2004).
10. M. Boehm, S. Martynov, B. Roessli, *et al.*, J. Magn. Magn. Mater. **250**, 313 (2002).
11. M. A. Popov, G. A. Petrakovskiĭ, and V. I. Zinenko, Fiz. Tverd. Tela (St. Petersburg) **46** (3), 478 (2004) [Phys. Solid State **46**, 491 (2004)].
12. M. Martinez-Ripoli, S. Martinez-Carrera, and S. Carcia-Blanco, Acta Crystallogr. B **27**, 677 (1971).
13. I. E. Dzyaloshinskiĭ, Zh. Éksp. Teor. Fiz. **47** (3), 992 (1964) [Sov. Phys. JETP **20**, 573 (1964)].
14. T. Moriya, Phys. Rev. **120**, 91 (1960).
15. J. S. Smart, *Effective Field Theories of Magnetism* (Saunders, London, 1966; Mir, Moscow, 1968).
16. Yu. A. Izyumov, *Diffraction of Neutrons on Long-Period Structures* (Énergoatomizdat, Moscow, 1987) [in Russian].
17. K. P. Belov, A. K. Zvezdin, A. M. Kadomtseva, and R. Z. Levitin, *Orientation Transitions in Rare-Earth Magnets* (Nauka, Moscow, 1979) [in Russian].

Translated by G. Tsydynzhapov